Using Attractor Behavior to Evaluate Neural Network Temperature Accuracy in World Cities

Huidong Tang[1], Yuichiro Mori[2] and Masahiko Toyonaga[2]
Graduate School of Integrated Arts and Sciences [1], Kochi University, Kochi 780-8520 Japan
Faculty of Science and Technology[2], Kochi University, Kochi 780-8520 Japan

Abstract

While neural network systems for temperature estimation have been based on an enormous number of nodes and connections and have provided accurate predictions, they are too large to implement in cheaper Internet of Things (IoT) systems. To address this, our previous work proposed combining a small neural network with temperature attractor behavior. Our small neural network mainly calculated stable temperature predictions, with attractor behavior detecting irregular temperatures. The results of our yearly experiments in Japanese cities showed that this method can accurately predict temperatures as well. In this paper, meanwhile, we verified the scope of our method's application by performing additional experiments in 12 cities worldwide. The results endorse the usefulness of our method.

1. Introduction

The White Paper on Information and Communications in Japan [1] states that the recent years have seen Japanese society reach Society 5.0, which highlighted the importance of systems that highly integrate cyberspace and vast real-world data (cyberphysical systems). Society 5.0 is the successor to the information society (Society 4.0), the industrial society (Society 3.0), the agrarian society (Society 2.0), and the hunter-gatherer society (Society 1.0). Related keywords include "artificial intelligence," "IoT," "big-data analysis," and "cloud computing."

Smart grids, one of the goals of Society 5.0, are being investigated in terms of their role in improving energy efficiency via energy distribution optimization. They quantify the energy in power grids and transmit power from surplus areas to demand areas, which necessitates the prediction of power consumption. However, challenges arise in such predictions because power demand may increase or decrease depending on highly correlated environmental factors such as temperature. Therefore, electricity demand estimation depends on maximum temperature (i.e., electricity demand is considered the maximum power consumption in any season). Hence, the ability to predict hourly temperatures would considerably reduce power consumption.

Traditionally, scientists have based their daily temperature approximations on simple statistical methods and long-term computer simulations [2]. However, they have focused their predictions only on maximum temperatures but not hourly temperatures, as temperature is part of a complex system that follows fluid dynamics.

Scholars have proposed several neural networks to forecast the weather [3–10]. Maximum temperature–related works are [3] and [6] while hourly temperature–related studies include [4], [5], and [7]. Maqsood et al. [4] proposed a 24-hour temperature prediction method, but its neural networks required large-scale memory and long learning times. Arun et al. [5] presented an hourly temperature prediction model but only calculated extremely short-term relations between temperature and time at one-hour intervals. Hayati et al. [7] created an hourly temperature prediction method, but it performed calculations at three-hour gaps. These show the lack of a round-the-clock hourly prediction technique via a small neural network that may be useful for small local power companies.

Although studies have suggested several small-scale neural networks, they only estimate maximum and minimum temperatures [11]. Thus, to determine the exact amount of electricity demand, predicting temperature transitions over time is crucial. Therefore, we proposed a small-scale neural network for forecasting temperature variations. We applied this system in five representative Japanese cities and achieved high accuracy, with errors ranging from 1.62% to 3.24%, but a rather wide error variance between cities.

In other fields, the stability of nonlinear systems has been studied using stock analysis [12], particularly range limitations of price movement, and some unconventional attractors have been identified that are known to affect price predictions [13]. These researchers found similarities between attractor bursts and the volatility clustering of empirical financial time series [14], which make it possible to predict rapid stock price changes by observing attractor bursts.

Our previous work described a novel temperature prediction method that combined a small neural

 DOI: 10.20533/ijicr.2042.4655.2021.0131

network and attractor behaviors. Our small neural network mainly predicted stable temperatures, and our attractor behaviors detected temperature fluctuations. The results of our yearly experiments in five major Japanese cities showed that this method can accurately predict temperatures in the country.

To verify our scope of application, we conducted additional experiments in 12 cities worldwide, whose further results validate the usefulness of our method. The next section describes the literature on temperature predictions and attractor behaviors. Section 3 explains our proposed method, which consists of a simple neural network and temperature attractor burst detection. Section 4 shows the experimental results of the relation between temperature attractors over time and temperature approximation errors. Section 5 concludes the paper.

2. Related work

2.1. Temperature estimation by mathematical formulae

The Japan Meteorological Agency (JMA) forecasts temperature and provides other information based on numerical predictions and past observations. Its forecasting calculations use neural networks, Kalman filters, logistic regression, and multiple linear regression (MLR). Before 1995, the JMA primarily used MLR but could not change its forecast model equation because MLR coefficients are fixed; if they did change the equation model, their forecast characteristics and accuracy would significantly deteriorate. In addition, these predictive model equations have certain drawbacks such as the use of long-term weather data, which complicates the reporting of annual and seasonal variations. Therefore, the JMA recently introduced continuous learning methods that accommodate improvements in neural networks, Kalman filters, and numerical prediction models to improve forecast accuracy.

2.2. Temperature estimation by neural networks

Several scholars have proposed temperature estimation techniques using neural network models to reflect recent weather conditions. These mathematical models represent neural connections in the brain, where neurons are modeled as nodes (points) and neural circuits as edges. Moreover, neural networks have the advantage of linking unknown nonlinear phenomena. Therefore, they can represent relations between unformulated data of input and output variables by tuning multiple variable coefficients.

Abhishek et al. [2] introduced a neural network model to approximate the highest and lowest temperatures of the day. Its structure consists of layer and node count as well as various transfer functions. This model makes it possible to report data covering long periods, such as annual and seasonal variations. The researchers claimed that the model had an accuracy of 0.211 deg^2 in mean square error (MSE) when it was allowed to learn the daily maximum temperature for a decade year at a specific Canadian location.

In addition, Maqsood et al. [4] constructed a learning and evaluation model combining multiple neural networks and using multiple parameters (e.g., temperature, humidity, and wind speed). They asserted that hourly temperature variations can be more accurately estimated through the mean of multiple neural networks. However, the model's excessive number of nodes, connections, and parameters result in long training and evaluation times.

To the best of our knowledge, no studies have evaluated hourly temperature transitions in small neural networks. Therefore, we developed a method to approximate hourly temperature changes in a small neural network that may be useful for small local contractors (e.g., agriculture and local power companies) [15]. The method produces low errors ranging from 1.62% to 3.24% in five representative Japanese cities. Section 3 discusses the model in detail.

2.3. Attractor behavior

Since temperature is a component of a complex system, it is well-known for its tendency to obey attractors. Hence, detecting the behavior of attractors would lead to more accurate predictions. However, since temperature transition is observed as a one-dimensional phenomenon, we need a method to transform it into three-dimensional transitions.

Iseri et al. [12] stated that an embedding theorem is an important method associated with nonlinear time series and chaos theory. They demonstrated that a single measured variable $x(n) = x(t_0 + n\tau)$ with t_0, some starting time, and τ sampling time, and its delays provide an *N*-dimensional space that serves as a proxy for the full multivariate state-space for the observed system. The *N*-dimensional state vectors $X(t)$ are then defined as:

$$X(t) = [x(t), x(t+\tau), \cdots, x(t+(N-1)\tau)] \quad (2.1)$$

where $x(t)$ is a time series value at time *t*, τ is a suitable time delay (sampling time), and N is the embedding dimension. This vector fully represents nonlinear dynamics at a large enough *N*. The embedding theorem guarantees that the time series of any measurement contains full knowledge of the behavior in a system and can be used to construct a proxy for the full multivariate phase space. This

 DOI: 10.20533/ijicr.2042.4655.2021.0131

requires state-space recognition at time delay τ and embedding dimension *N*.

They [12] used a one-dimension time series $x(t_0), \cdots, x(t_i), \cdots, x(t_n)$ and extended it to a phase type of an *m*-dimensional phase space:

$$\begin{matrix} X(t_0) & \cdots & X(t_i) & \cdots & X(t_n) \\ X(t_0+\tau) & \cdots & X(t_i+\tau) & \cdots & X(t_n+\tau) \\ X(t_0+2\tau) & \cdots & X(t_i+2\tau) & \cdots & X(t_n+2\tau) \\ \vdots & \vdots & \vdots & \vdots & \vdots \\ X(t_0+(m-1)\tau) & \cdots & X(t_i+(m-1)\tau) & \cdots & X(t_n+(m-1)\tau) \end{matrix} \quad (2.2)$$

where $\tau = k\Delta t (k = 1,2,\cdots)$ denotes delay time, and a phase point of the phase space consists of *every* row in equation (2.2). Each phase point $X(t_i)$ has *m* weights, $X(t_i), X(t_i+\tau), \cdots, X(t_i+(m-1)\tau)$.

Every phase point of the *m*-dimensional phase space embodies a certain instantaneous state, and their phase space trajectory consists of their link-line in which the system state evolves with time. System dynamics can then be studied in more phase space dimensions. In this paper, we used this method to generate attractors.

3. A tiny neural network and an attractor

3.1. Proposed neural network model

We proposed an extremely small neural network model, called a tiny neural network, as a small-scale, short-term learning method for temperature estimation [15].

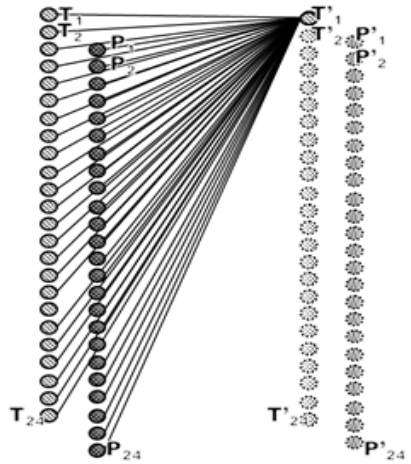

Figure 1. Tiny neural network for 24-hour temperature estimation

The Figure 1 illustrates our proposed neural network, which consists of two layers, an input layer and a fully connected layer, where the nodes modeling the neurons are stratified and connected. The input layer has 24 × 2 nodes, with the observed hourly temperature data from T_1 to T_{24} and the observed pressure data from P_1 to P_{24} in a day. Each node has its value, and the value of each edge is the weight. The *i*-th output temperature node T'_i is connected to all input nodes from T_1 to T_{24} and from P_1 to P_{24} with weighted edges. The *i*-th output pressure node P'_i is also connected to all input nodes from T_1 to T_{24} and from P_1 to P_{24} with weighted edges.

Note that the input temperatures from -50 to 50 degrees [Celsius] and the input pressures from 900 hPa to 1100 hPa are both normalized from 0 to 1. The teacher values are normalized similarly.

3.2. Estimation of the next 24-hour temperature transition

The training of the proposed network model's weights is shown in pseudo-code in Figure. 2. Its input consists of 24-hour temperature and pressure data for several days as well as the initial values of the network's weight, and its output is the weight of the trained network.

First, the 24-hour temperature and pressure data, as inputs to the proposed network model, allows for the calculation of the 24-hour output and the sum of squared errors with the 24-hour data for the next day (teacher data). The weights are adjusted via the steepest-descent method so that the sum of the squared errors becomes the minimum. The number of training times is repeated, and then the number of epoch times is repeated for several days as well. The resulting weight is output as the trained network's weight. The neural network model harnesses the data for a particular day and the weights of the trained network to approximate both the temperature and pressure for the next 24 hours.

This system requires the above training procedure for each region where temperature and pressure are measured.

```
Teaching procedure

for(epoch times){
  for(input days){
    Enter temperature and pressure data of a day
    for(training times){
      Calculate 24 hour output
      Calculate the sum of the squared error
        with 24 hour teach-data
      Adjust the weights by the steepest descent method
        to minimize the sum of the squared errors.
    }
  }
}
```

Figure 2. Tiny neural network training procedure

3.2. Attractor behavior

Studies have examined the stability of nonlinear systems in stock analysis [12], specifically the range

 DOI: 10.20533/ijicr.2042.4655.2021.0131

limitations of the price movement phenomenon, and have observed some unconventional attractors. These attractor shapes are known to influence price predictions [13]. Researchers have also observed similarities among the attractor bursts and volatility clustering of empirical financial time series [14] (i.e., rapid changes in stock prices may be forecast by observing attractor bursts). Therefore, we aimed to improve temperature estimation accuracy by reflecting attractor bursts of temperature in the proposed neural network.

We assigned the three-dimensional point (x(t), y(t), z(t)) with T_t = v(t) (temperature at t-th o'clock) as x(t). Let T_{t+1} = v(t+1) (temperature at t+1-th o'clock) be y(t) and T_{t+2} = v(t+2) (temperature at t+2-th o'clock) be z(t) on the same day and embed the other points the same way until 22-th o'clock. Figure. 3(a) and 3(b) show temperature transitions and their corresponding attractors. The temperature transition attractor consists of a three-dimensional phase space, as shown in Figure 3(c).

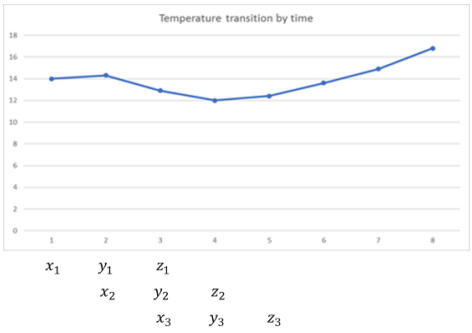

(a) A sample of a temperature transition

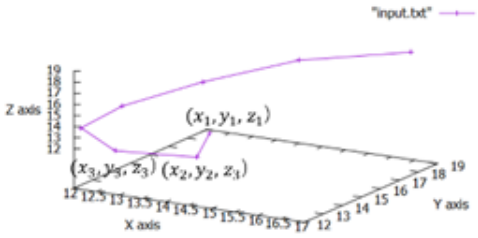

(b) Temperature attractor corresponding to (a)

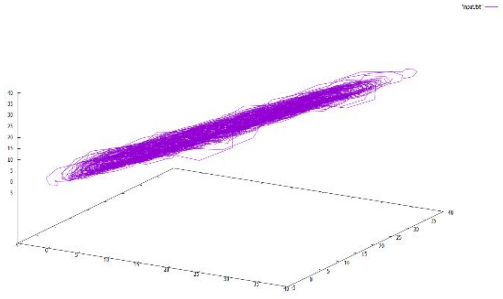

(c) Temperature transition attractor

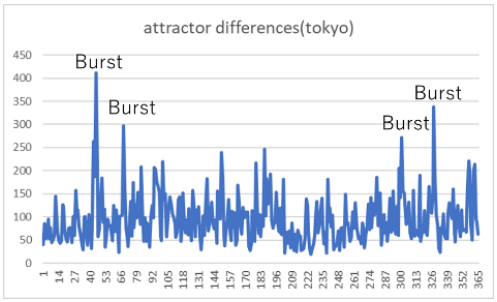

(d) Temperature attractor distance bursts

Figure. 3. Temperature attractors and their bursts

In our proposed method, we assumed that, if the distance from one point to another in Figure. 3(c) is longer than other distances, an anomaly can be detected as a point in the vicinity, called a burst. To detect this burst, we plotted the values of Equation 3.1, which calculates the distance between the points, in Figure. 3(d), which indicates the presence of some obviously longer distances. We can presume that predictions are difficult at these locations. Therefore, we thought that we could exclude these locations to provide a stable estimate [17].

The difference d^J between the J-th day and J+1-th day is the sum of the 22-hour Euclidean distance as in equation (3.1).

$$d^J = \sum_{t=1}^{22} \sqrt{\left(x^{J+1}(t) - x^J(t)\right)^2 + \left(y^{J+1}(t) - y^J(t)\right)^2 + \left(z^{J+1}(t) - z^J(t)\right)^2} \quad (3.1)$$

where $x(t) = v(t)$, $y(t) = v(t+1)$, $z(t) = v(t+2)$

The Figure 3(d) shows relatively violent bursts of the attractor in Figure. 3(c). These bursts are parts of an attractor where irregular oscillations occur amid regular ones from time to time.

Accuracy detection by attractor behavior

Step1. calculate A(t) and A(t+dt)
Step2. calculate distance d(t) = |A(t) - A(t+dt)|
Step3. if(d(t)> C)then alert the estimation
else show the estimation

Figure 4. Accuracy estimation by attractor behavior

4. Experiment

4.1. Purpose and data

To verify the estimation errors of the 24-hour temperature and atmospheric pressure transition via the proposed neural network model, analysis was performed using hourly air temperature and

DOI: 10.20533/ijicr.2042.4655.2021.0131

atmospheric pressure data from various areas in Japan, named dataset 1 [17].

Dataset 1 consists of the north and south of Japan, such as Sapporo, Tokyo, Kyoto, Kochi, and Naha. Data from 2009 to 2015 served as learning data while data from 2016 were used as evaluation data. The data employed by the JMA are available on their website. We selected these cities because they are geographically separate from one another in latitude; therefore, they represent a wide range of climatic conditions in Japan. The outline is shown below:

[Dataset 1 overview]
Learning data: hourly temperature and pressure from 2009 to 2015.
Evaluation data: hourly temperature and pressure in 2016.
Data locations: Sapporo, Tokyo, Kyoto, Kochi, Naha.
Data source: JMA (downloaded on October 31, 2019).

In this paper, to verify the scope of our method's application, we performed additional experiments in the same five cities in Japan and seven other cities in the United States, Canada, and Israel, named datasets 2 and 3, respectively.

Dataset 2 consists of the same cities in dataset 1. Data from 2012 to 2018 served as learning data, and data from 2019 were used as evaluation data. The data employed by the JMA can be accessed from their website. We selected the same cities because we intended to compare datasets 1 and 2. Below is the outline.

[Dataset 2 overview]
Learning data: hourly temperature and pressure from 2012 to 2018.
Evaluation data: hourly temperature and pressure in 2019.
Data locations: Sapporo, Tokyo, Kyoto, Kochi, Naha.
Data source: JMA (downloaded on December 10, 2020).

Dataset 3 is composed of the northern and southern United States (Seattle, New York, Atlanta, and Miami), Canada (Toronto), and Israel (Jerusalem and Eilat). Data from 2013 to 2015 served as learning data while data from 2016 were used as evaluation data. The hourly weather data for 30 U.S. and Canadian cities and 6 Israeli cities [16] are available online. Dataset 3 was also selected for the cities' geographical separation in terms of latitude. The outline is shown as follows.

[Dataset 3 overview]
Learning data: hourly temperature and pressure from 2013 to 2015.
Evaluation data: hourly temperature and pressure in 2016.
Data locations: Seattle (USA), Toronto (Canada), New York (USA), Atlanta (USA), Jerusalem (Israel), Eilat (Israel), and Miami (USA).
Data source: Hourly weather data for 30 U.S. and Canadian cities and 6 Israeli cities. [16]

4.2. Experimental conditions

Here are the experimental conditions of our neural network model:

- The epoch is 100 times, and the training is 100 times per 1-day, 24-hour data.
- The initial learning rates of training are 10^{-1}, 10^{-2}, 10^{-3}, 10^{-4}, and 10^{-5}, and the reduction rates per epoch iteration are $10^{-0.01}$, $10^{-0.02}$, and $10^{-0.03}$.
- The neuron activation function is Rectified Linear Unit (ReLU).

Learning was conducted by gradually updating the connection weights with the learning rate per training time and repeating it several times per day. The learning rate dropped with the reduction rate per epoch time, which was repeated several times over the entire training data.

The activation function was used to calculate the node output. ReLU was employed in this two-dimensional, connection-limited neural network model. The 24 × 2 nodes of the fully connected layer were compared with those of a teach layer, whose temperatures from -50 to 50 degrees [Celsius] and pressures from 900 hPa to 1100 hPa were both normalized from 0 to 1.

4.3. Results for Japanese cities in 2016 and 2019

The learning and epoch iteration numbers were both fixed at 100. The initial learning rate and its reduction rate per epoch iteration are 10^{-3} and $10^{-0.03}$, respectively, which are the best parameters for Kochi temperature estimation.

We estimated the next day temperature transition from the previous-day temperature transition in 2016 using dataset 1 in five Japanese cities—Sapporo, Tokyo, Kyoto, Kochi, and Naha. The learning period was seven years. And also approximated the next day temperature transition from the previous-day temperature transition in 2019 using dataset 2 in the same five cities in Japan. The learning period was also seven years.

Table 1 shows the mean absolute percentage errors (MAPEs) between the observed and estimated 24-hour next day temperature transitions over 365 days, one for 2016 and one for 2019. It displays the errors for Sapporo, Tokyo, Kyoto, Kochi, and Naha in 2016

 DOI: 10.20533/ijicr.2042.4655.2021.0131

(3.24%, 2.80%, 2.64%, 2.27%, and 1.62%, respectively) and 2019 (3.46%, 2.86%, 2.55%, 2.29%, and 1.55%, respectively).

Table 1. MAPEs (%) of the 24-hour temperature transitions in five Japanese cities in 2016 and 2019

Cityies	2016	2019
Sapporo	3.24	3.46
Tokyo	2.8	2.86
Kyoto	2.64	2.55
Kochi	2.27	2.29
Naha	1.62	1.55

The worst MAPEs in 2016 (3.24%) and 2019 (3.46%) in our hourly temperature estimations are comparable with literature findings (3.2%) [7], where the interval time is three hours. The MAPEs in 2019 are comparable with those in 2016; hence, we believe that our model can be used in different years in Japan.

4.4. Results for seven cities in three other countries

We fixed both the learning and epoch iteration numbers at 100. The initial learning rate and its reduction rate per epoch iteration are 10^{-3} and $10^{-0.03}$, respectively; they are the best parameters for Kochi temperature estimation. And estimated the next day temperature transition from the previous-day temperature transition in 2016 in seven cities in the United States (Seattle, New York, Atlanta, and Miami), Canada (Toronto), and Israel (Jerusalem and Eilat). The learning period was three years.

Table 2. MAPEs (%) of 24-hour temperature transitions in seven cities in three countries in 2016

Cityies	2016
Seattle(USA)	2.88
Toronto(Canada)	4.33
New York(USA)	3.35
Atlanta(USA)	4.54
Jerusalem(Israel)	2.31
Eilat(Israel)	2.88
Miami(USA)	3.18

Table 2 shows the MAPEs between the observed and approximated 24-hour next day temperature transitions for 365 days in 2016. Table 2 displays the errors in that year for Seattle, Toronto, New York, Atlanta, Jerusalem, Eilat, and Miami (2.88%, 4.33%, 3.35%, 4.54%, 2.31%, 2.88%, and 3.18%, respectively).

The results are slightly worse than those in Japan, which may be due to geographical factors or the shorter learning period.

4.5. Neural network evaluation error and attractor difference comparison

Figure. 5(a)–(e) plot the comparisons between estimation errors by our neural networks and the attractor bursts in Sapporo (Hokkaido), Tokyo (Kanto), Kyoto (Kinki), Kochi (Shikoku), and Naha (Okinawa) in 2016. The dotted squares in each figure are the dates of the larger estimation errors and attractor differences (i.e., burst points). These points show a clear correlation with each other.

Figure. 6(a)–(c) show the comparison plots for the estimation errors by our neural networks and the attractor bursts in Toronto, Eilat, and Miami in 2016. The dotted squares in each figure indicate the dates of the larger estimation errors and attractor differences (i.e., burst points). These points also show clear correlations with each other except Toronto.

Thus, if we avoid approximating at the attractor burst dates, we can estimate a temperature transition much more accurately. Therefore, we have proposed an algorithm, shown in Figure. 4. Nevertheless, it was difficult to explain why Toronto's estimation errors and attractor bursts are not correlated with each other. Furthermore, estimating a specific burst date also remained a challenge. One possible solution may be to use a tiny neural network to estimate burst dates by training the attractors.

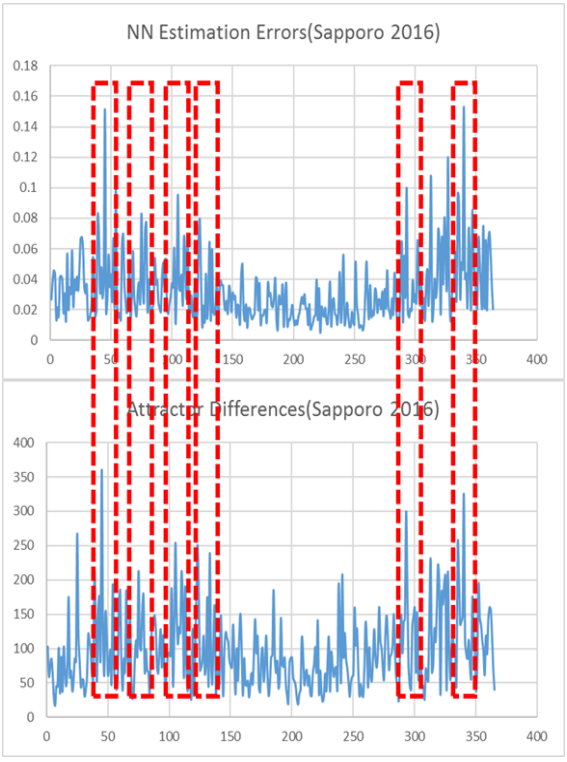

(a) Comparison between estimation errors and attractor bursts in Sapporo

DOI: 10.20533/ijicr.2042.4655.2021.0131

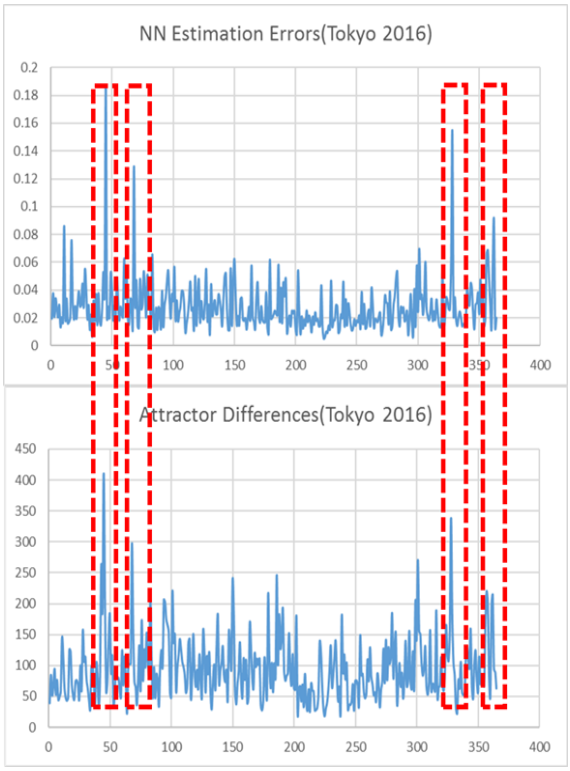

(b) Comparison between estimation errors and attractor bursts in Tokyo

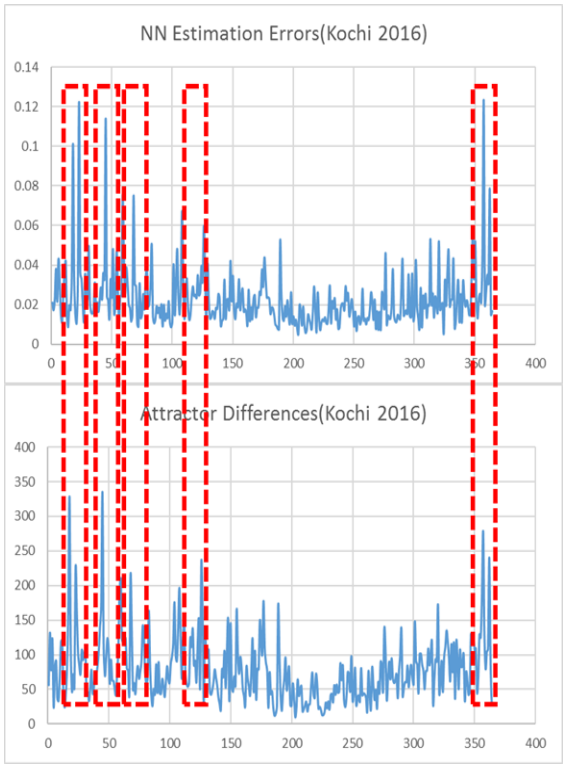

(d) Comparison between estimation errors and attractor bursts in Kochi

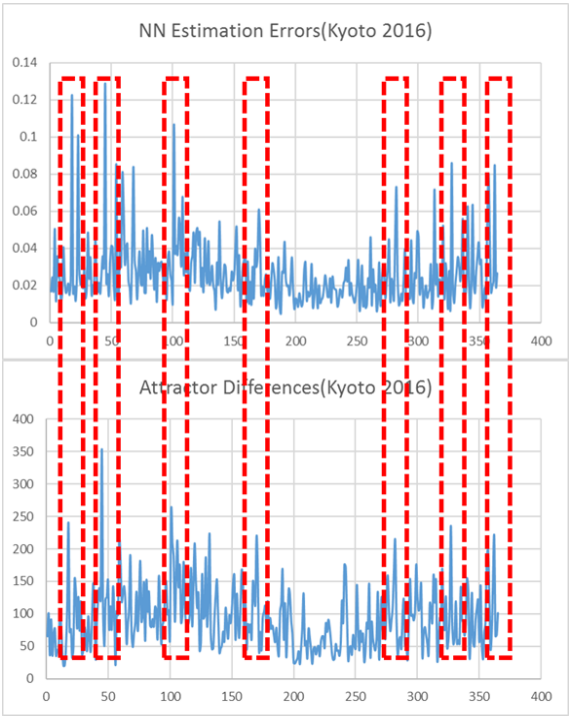

(c) Comparison between estimation errors and attractor bursts in Kyoto

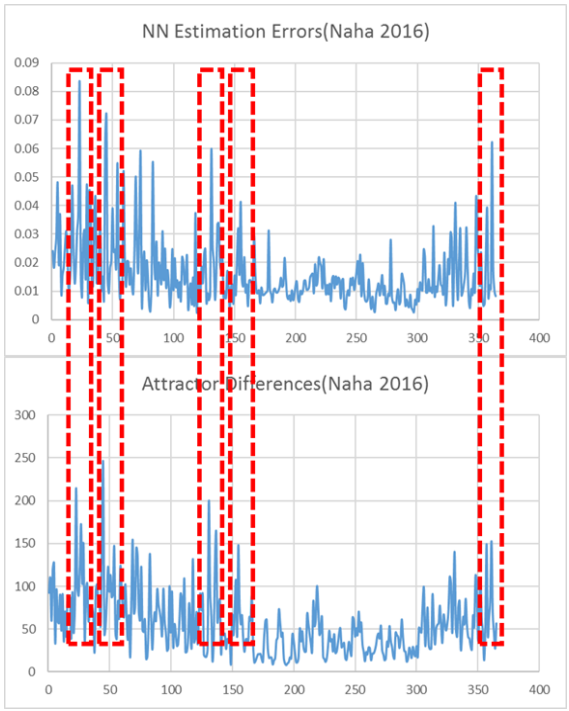

(e) Comparison between estimation errors and attractor bursts in Naha

Figure 5. Comparisons between estimation errors and attractor bursts in Japanese cities

DOI: 10.20533/ijicr.2042.4655.2021.0131

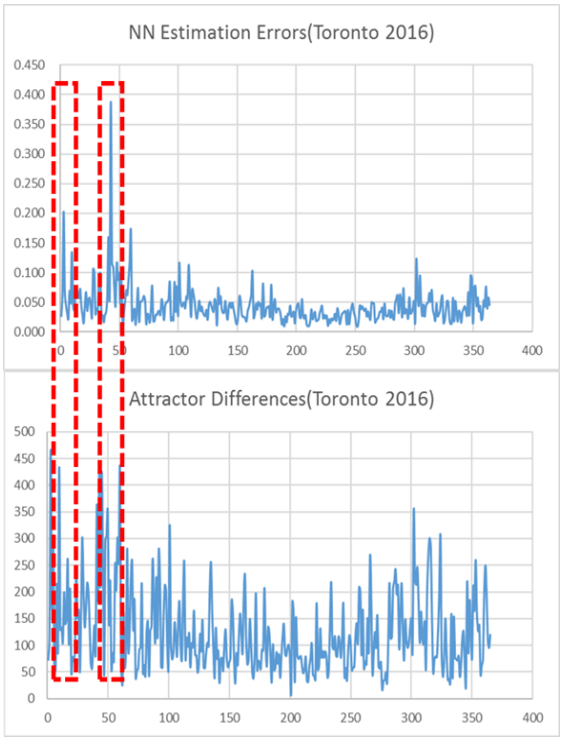

(a) Comparison between estimation errors and attractor bursts in Toronto

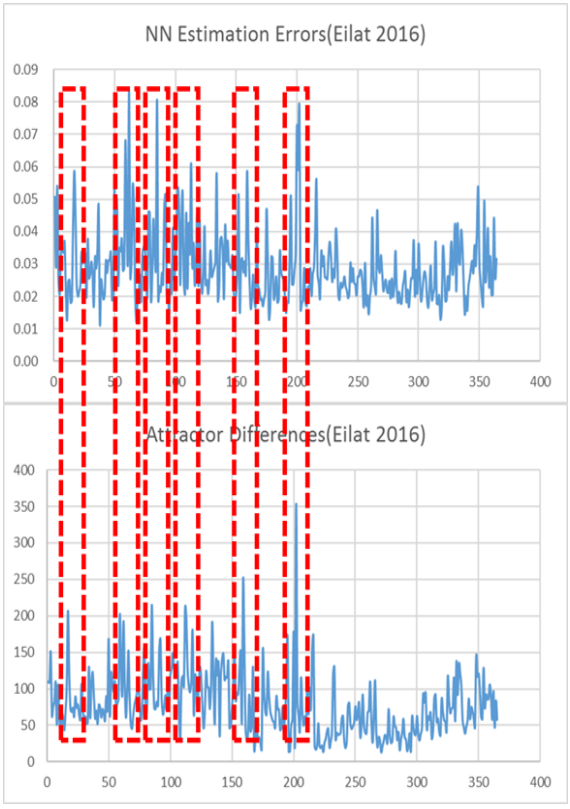

(b) Comparison between estimation errors and attractor bursts in Eilat

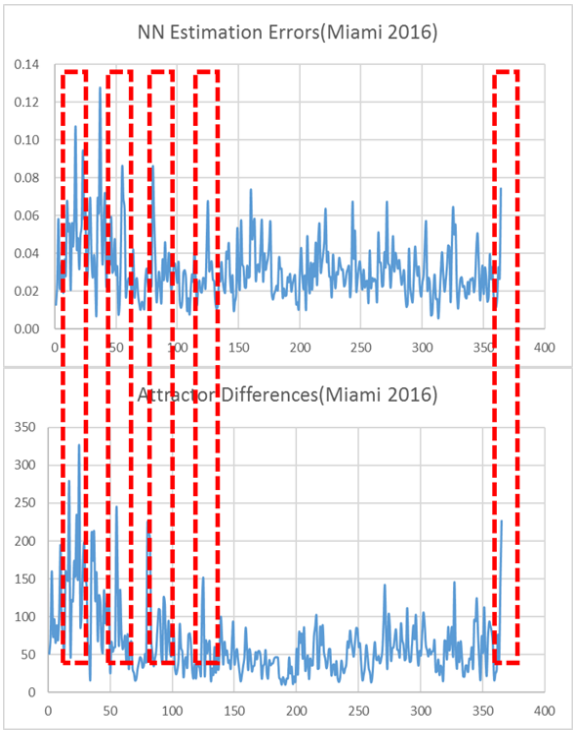

(c) Comparison between estimation errors and attractor bursts in Miami

Figure 6. Comparisons between estimation errors and attractor bursts in Canada, Israel, and United States

5. Conclusion

In our previous work, we proposed a method for improving neural network estimation accuracy using attractor behavior. While existing neural network models mainly aim for accurate estimations of temperature transitions, we have focused on incorporating the attractor bursts of these transitions, finding strong correlations between estimation errors and attractor bursts. Our new method, which combines a simple neural network and temperature attractor behaviors, managed to predict accurate temperatures in Japan.

To confirm our method's scope of application, we performed additional experiments in five cities in Japan in 2019 and in seven cities in the United States, Canada, and Israel in 2016. The Japanese cities' MAPEs in 2019 were comparable with their MAPEs in 2016, but the MAPEs of seven cities outside Japan were slightly worse than those in Japan. These results validated the usefulness of our method. We plotted the comparisons between estimation errors and attractor bursts for Toronto, Eilat, and Miami in Canada, Israel, and the United States, respectively, in 2016, and found clear correlations between estimation errors and attractor bursts except for Toronto.

However, one challenge in our future work would be to explain the lack of correlation between the

 DOI: 10.20533/ijicr.2042.4655.2021.0131

estimation errors and attractor bursts in Toronto. Approximating specific burst dates remains a challenge as well, but attractor training may be one possible solution to this.

6. References

[1] Ministry of Internal Affairs and Communications, (2014). White Paper information and communications in Japan, Published by the Government of Japan.

[2] Abhishek K., Singh M. P., Saswata G., Abhishek A., (2012). Weather forecasting model using artificial neural network, Procedia Technology, 4: 311-318.

[3] Baboo S. S., Shereef I. K., (2010). An efficient weather forecasting system using artificial neural network, International Journal of Environmental Science and Development, 1.4: 321.

[4] Maqsood I. Khan, Muhammad R., Abraham A., (2004). An ensemble of neural networks for weather forecasting, Neural Computing and Applications, 13.2: 112-122.

[5] Arun S. L, Selvan M. P., (2016). Very short-term prediction of solar radiation for residential load scheduling in smartgrid, In National Power Systems Conference (NPSC), IEEE, 1-5.

[6] Paras S. M, Kumar A, Chandra M., (2009). A feature based neural network model for weather forecasting, International Journal of Computational Intelligence, 4.3: 209-216.

[7] Hayati M, Mohebi Z., (2007). Application of artificial neural networks for temperature forecasting, World Academy of Science, Engineering and Technology, 28.2: 275-279.

[8] Bustami R., Nabil B., Charles B., Suhaila S., (2007). Artificial neural network for precipitation and water level predictions of bedup river, IAENG International Journal of Computer Science, 34.2.

[9] Hall T., Brooks H. E., Doswell III C. A., (1999). Precipitation forecasting using a neural network, Weather and Forecasting, 14.3: 338-345.

[10] Hung N. Q., Babel M. S., Weesakul S., Tripathi N. K., (2009). An artificial neural network model for rainfall forecasting in Bangkok, Thailand, Hydrology and Earth System Sciences, 13.8.

[11] Parton W. J., Logan J. A., (1981). A model for diurnal variation in soil and air temperature, Agricultural Meteorology, 23: 205-216.

[12] Iseri M., Caglar, Hikmet C. N., (2008). A model proposal for the chaotic structure of Istanbul stock exchange, Chaos, Solitons and Fractals, 36.5: 1392-1398.

[13] Hanias M. P., Curtis G. P., Thallasinos J. E., (2007). Non-linear dynamics and chaos: The case of the price indicator at the Athens Stock Exchange, International Research Journal of Finance and Economics, 11.1: 154-163.

[14] Krawiecki, A., Hołyst, J. A., Helbing, D., (2002). Volatility clustering and scaling for financial time series due to attractor bubbling, Physical Review Letters, 89.15: 158701.

[15] Tang H., Mori, Y., Toyonaga M., (2020). A tiny neural network model for estimating next 24-hour temperature transition, In the Proceedings of ICSSE, pp 274-279.

[16] Beniaguev D., "Hourly weather data for 30 US and Canadian Cities and 6 Israeli Cities", https://www.Kaggle.com/selfishgene/historical-hourly-weather-data (Access Date: 10 December, 2020).

[17] Tang H., Mori Y., Toyonaga M., (2020). A Method for Evaluating the Accuracy of Neural Network Estimation Using Attractor Behavior, In the Proceedings of WCST, to be published.

7. Acknowledgements

The authors would like to thank Enago (www.enago.jp) for the English language review.

